Med Chem Res (2016) 25:2410–2424
DOI 10.1007/s00044-016-1647-2

MEDICINAL CHEMISTRY RESEARCH

ORIGINAL RESEARCH

Homology modeling of chemokine CCR7, molecular docking, and in vitro studies evidenced plausible immunotherapeutic anticancer natural compounds

Pushpendra Singh[1] · Ravi Shankar Singh[2] · Alka Rani[1] · Felix Bast[1]

Received: 10 July 2015 / Accepted: 4 July 2016 / Published online: 4 August 2016

Abstract The chemokine receptor 7 is a G-protein coupled, receptors coordinates the migration of cancer cells towards CCL19 and CCL21 constitutively expressed lymphatic organs. Chemokine receptor 7 facilitates cancer progression by generating new lymphatic vessels that serve as conduits for tumor dissemination to lymph nodes. In this context, chemokine receptor 7 inhibitor recently caught an attention for cancer cell growth inhibitor. The 3-D crystalline structure of chemokine receptor 7 not available in protein data bank (PDB), first we predicted the 3-D structure of chemokine receptor 7 and then performed receptor-based molecular docking of chemokine receptor 7 against natural and marine compounds. Semiquantitative polymerase chain reaction (PCR) and quantitative real-time PCR were performed for mRNA expression of chemokine receptor 7 and glyceraldehyde 3-phosphate dehydrogenase (GAPDH) used as internal control. The best-docked compounds have been selected for chemokine receptor 7 inhibitors by optimal energy value (Gscore), types of interactions, and conformations. CID6441009, 42607750, 72276, 6711419, 56835050, 65064, 23663412, 72277, 643668, 54679285 compound have a better binding energy −11.35, −10.51, −10.16, −9.98, −9.95, −9.86, −9.83, −9.57, −9.47, and −9.45 respectively against chemokine receptor 7. Protein–ligand interactions profile highlighted that amino acid Glu45, Lys50, Arg54, Lys57, Trp114, Met260, Glu205, Gln227, Gln276, and Asp309 involved in the hydrophobic, hydrogen bonding, and π-π stacking interactions play a central role at the active site. Moreover, treatment with the Epigallocatechin gallate led to down-regulation of mRNA expression of chemokine receptor 7 in HepG2 and PC3 cells. This molecular docking study recapitulates the docking free energy, protein—ligands interactions profile, pharmacokinetic, and the pharmacodynamic parameter of lead molecules, which are extremely helpful to improve the activity of natural and marine compounds against chemokine receptor 7.

Keywords Natural compounds · Cancer · In silico · Maestro 9.6 · In vitro

Introduction

Chemokines are small molecular weight secreted proteins, which activates signaling pathway involved in tumor cell dissemination, migration and metastasis formation after binding to chemokines receptors, thus may influence cancer development and progression. Chemokine receptor 7 (CCR7) are chemoattractant protein that expressed by variegated cancer cells, such as non-small lung cancer, gastric cancer, and esophageal cancer (Ding et al., 2003; Mashino et al., 2002; Takanami, 2003). Moreover, numerous studies have shown that CCR7 and its ligand (CCL19), stimulates cell proliferation, migration, and invasion in prostate, bladder and hepatocellular cancer (Chen et al., 2015; Cunningham et al., 2010; Mo et al., 2015; Peng, Zhou, An and Yang, 2015; Schimanski et al., 2006). The recent study

✉ Felix Bast
felix.bast@gmail.com
felix.bast@cup.ac.in

[1] Centre for Biosciences, School of Basic and Applied Sciences, Central University of Punjab, Bathinda, Punjab 151001, India

[2] Department of Molecular Medicine & Biotechnology, Sanjay Gandhi Post Graduate Institute of Medical Sciences, Lucknow 226014, India

showed that malignant cells use chemokine receptor/ligand interactions that ameliorated to the metastatic process. Consequently, it was found that the expression of CCR7 in the various tumor that responded by various cytokines, led to cancer metastasis (Chen et al., 2015). In contrast, co-expression of the epidermal growth factor receptor (EGFR) with CCR7 in breast cancer has been associated with a poor prognosis.

A plethora of monoclonal antibodies has entered into clinical trials that inhibit the chemokines activity, due to their long half-life in blood, and high affinity specific interactions with low toxicity. However, it is complicated and expensive, to develop and produce monoclonal antibodies, in addition to less convenient to route of administration than small compounds. Moreover, various small molecular inhibitor such as CXCR4 (burixafor MSX-122, CTCE-9908, and BKT140) (Debnath et al., 2013; Peled et al., 2013), CCL2–CCR2 (cenicriviroc, PF-4136309, and MK-0812) (Sanford et al., 2013), and CCR5 (Maraviroc) have discovered and entered in to cancer clinical trials (Adams et al., 2015). But there is not any inhibitor of CCR7 is available, which is still under consideration.

The toxicity and severe side effects associated drug resistance with the current drugs have provided the much-needed impulsion for the establishment of new anticancer agents. Over the past many years, synthetic analogs of natural and marine compounds with improved potency, have been prepared, thus, portraying natural and marine compounds are model for cancer drug discovery (Biswas et al., 2006; Martin et al., 2007, 2011). Natural phenolic compounds modulate the protein expression of numerous biological processes including the cell cycle, apoptosis, and angiogenesis, make them promising agents in cancer research (Gray et al., 2014; Hayashi et al., 2008; Tabuchi et al., 2013). Therefore, in the present study, we have investigated the natural and marine compounds as inhibitors for CCR7 using in silico and in vitro approach.

Methodology

Selection and preparation of ligands

Grid-based Ligand Docking with Energetics (GLIDE) based molecular docking protocol adapted from our previous published literature (Singh and Bast, 2014a, b; Singh and Bast, 2015a, b, c). The database of 186 marine and natural compounds used as ligands in our molecular docking studies was derived from diverse medicinal plant extracts and marine organisms. These selected marine and natural compounds as a ligand molecules were well reported in the literature (Bhanot et al., 2011; Cherigo et al., 2015; Cho and Park, 2008; Cragg and Newman, 2005; da Rocha et al., 2001; Hillman, 2012; Huang et al., 2012; Mayer and Gustafson, 2004, 2006, 2008; Phosrithong and Ungwitayatorn, 2010; Roell and Baniahmad, 2011; Sarkar and Li, 2006; Sawadogo et al., 2015; Sawadogo et al., 2013). These ligand molecules were subjected to ligand preparation by Ligprep wizard application of the Maestro 9.6, that performs amendment on the ligands, such as the addition of hydrogen, 2D to 3D conversion, corrected bond lengths and bond angles, low energy structure, stereochemistry and ring conformations. Ligprep wizard protocol generated ten structures conformations for each compound. After preparation of ligands, energy minimization, optimization, and molecular dynamics was done by using optimized potential for liquid simulations (OPLS 2005) force field (Jorgensen et al., 1996; Jorgensen and Tirado-Rives, 1988; Shivakumar et al., 2010), and finally, ten conformations for each ligand was used for further study.

Homology modeling of CCR7 protein

For the design of rational targeted drugs, the 3-D crystalized structural information about the target is much important. When the 3D structure is not available in the protein data bank, the comparative homology modeling is the most precise method for prediction of protein structure by using in silico approach. Thus, the protein structure of CCR7 predicted by using the IntFOLD (Version 2.0) (McGuffin et al., 2008). For homology modeling, the protein sequence of the amino acids in CCR7 protein of *Homo sapiens* was obtained from GenBank database (GenBank: EAW60669.1).

Preparation of protein molecules, receptor grid formation, and GLIDE molecular docking

Protein was prepared using the Maestro 9.6 protein preparation wizard by addition of hydrogen atoms, assigning bond orders, creation of zero-order bonds to metal, creation of disulphide bonds, fixing of the charges, and orientation of groups. After preparing protein molecules, minimization and optimization were done using an OPLS2005-force field of Maestro 9.6. The active site of the protein molecules was determined by using receptor grid generation option of Maestro 9.6. We had generated the grid that covers the entire active residue cavity. Receptor grid was scaled by van der Waals radii of 1.0 Å with partial atomic charge less than 0.25 Å as the default setting of Maestro. Other parameters such as sites, constraints, and excluded volume, the default setting of the Maestro were used (Friesner et al., 2006; Repasky et al., 2007). The best fit compounds have been preferred for the target on the basis of optimal energy value (Gscore), type of interactions, potential for bonding, and conformations (Friesner et al., 2004; Halgren et al., 2004).

The Gscore was calculated in kcal/mol, and it was an accumulative energy of a number of parameters such as hydrogen bond, hydrophobic, van der waals, polar interactions in the binding site, metal binding term and penalty for buried polar groups and freezing rotatable bonds.

ADME/T (absorption distribution metabolism excretion and toxicity) studies

In silico prediction of ADME/T are the cooperative strategy that could abolish indecorous compounds, before investment of valuable time and money in the primary testing of compounds. Computer based theoretical approaches were described to be the best option for prediction of ADME of new compounds. The poor compound solubility, gastric emptying time, chemical instability in the stomach, and inability to permeate the intestinal wall can all diminish the extent to which a drug is absorbed after oral administration. Thus, ADME properties of best-docked compounds were predicted using QikProp application of Maestro. It predicts properties such as logBB, overall CNS activity, Caco-2, and MDCK cell permeability and logKhsa for human serum albumin binding, etc. which were essential for drug like pharmacokinetic profile (Jorgensen and Duffy, 2002; Lu et al., 2004).

Cell culture conditions and Epigallocatechin gallate (EGCG) treatment

Hepatocellular carcinoma (HepG2) and prostate cancer (PC3) were obtained from the NCCS, Pune (India). HepG2 cells were grown in phenol-red DMEM supplemented with 10 % heat-inactivated Fetal bovine serum (FBS), 1 % penicillin (100 units/ml), and streptomycin (100 mg/ml). PC3 cells were grown in Ham's F-12K medium supplemented with 10 % FBS, 1 % penicillin (100 units/ml), and streptomycin (100 mg/ml). All cells were maintained at 37 °C in a humidified atmosphere with 5 % CO_2 and were exposed to 80 µM EGCG for 48 hrs. Cells incubated with culture medium with an equivalent amount of vehicle DMSO (final DMSO concentration was <0.2 %) served as controls.

Total RNA isolation, cDNA synthesis, and quantitative RT-polymerase chain reaction (PCR)

One million cells/well were plated into the six well plates, culture media supplemented with 10 % FBS and 1 % penicillin streptomycin and incubated at 37 °C. Cells were exposed to 80 µM EGCG for 48 h, and total RNA was extracted using Trizol (Life Technologies, Gaithersburg, MD) according to manufacturer's instructions and previous reports from our lab (Singh and Bast, 2015a, b, c). RNA quantified at 260/280 nm with thermo scientific nanodrop 2000 spectrophotometer. The absorption ratio A260 nm/A280 nm between 1.90 and 2 was taken into consideration for cDNA preparation. Approximately, one microgram of total RNA was reverse-transcribed into cDNA using a high capacity PrimeScript 1st strand cDNA Synthesis Kit (Takara Bio Inc). Primers sequence of CCR7 were adapted from previously published article sense, 5′-CTCCAGG-CACGCAACTTTGA-3′ and antisense, 5′-CACAGGTGC-TACTGGTGATGTTGA-3′. Semiquantitative PCR and quantitative real-time PCR were performed using Veriti® 96-well fast thermal cycle and StepOnePlus™ Real-Time PCR System (SYBR green chemistry) respectively (Applied Biosystems) using glyceraldehyde 3-phosphate dehydrogenase (GAPDH) as an internal control. An expected amplified sequence of CCR7 was 145 bp fragment and real time data was analyzed by using 2^{-ddCt} method.

Result and discussion

Homology modeling of CCR7 protein by using IntFOLD server

The IntFOLD server is a self-regulating server that integrates several cutting-edge methods for the prediction of protein structure and function from amino acid sequence. The protein sequence of CCR7 (*Homo sapiens*) was retrieved from the PubMed database (GenBank: EAW60669.1) for protein model generation. Protein structure of CCR7 predicted by using the IntFOLD integrated protein structure and function prediction server (Version 2.0 Roche et al., 2011). The results Table is ranked according to the decreasing global model quality score. The predicted protein structures have global model quality scores range between 0 and 1. In general scores less than 0.2 indicate there may be incorrectly modeled domains and scores greater than 0.4 indicate more complete and confident models, which are highly similar to the native structure. Template selection is an imperative preliminary point in homology modeling because it determines the primary folding of the target structures and influences their quality. P00268 (Rubr clopa) Rubredoxin and P51681 (CCR5 human) was selected as a template for the prediction of CCR7 model. These models have a confidence and *p*-value CERT 5.493E-4 along with global model quality score is 0.7122. The quality of homology modeling of CCR7 protein determined using various parameters (Fig. 1). Model quality assessment is carried out using ModFOLDclust2 and predicted the per-residue error in angstroms as shown in Fig. 2(a). Disorder prediction plot detected from DISOclust 2.0. Figure 2(b) displays a plot of the probability of disorder (on the y-axis) for each

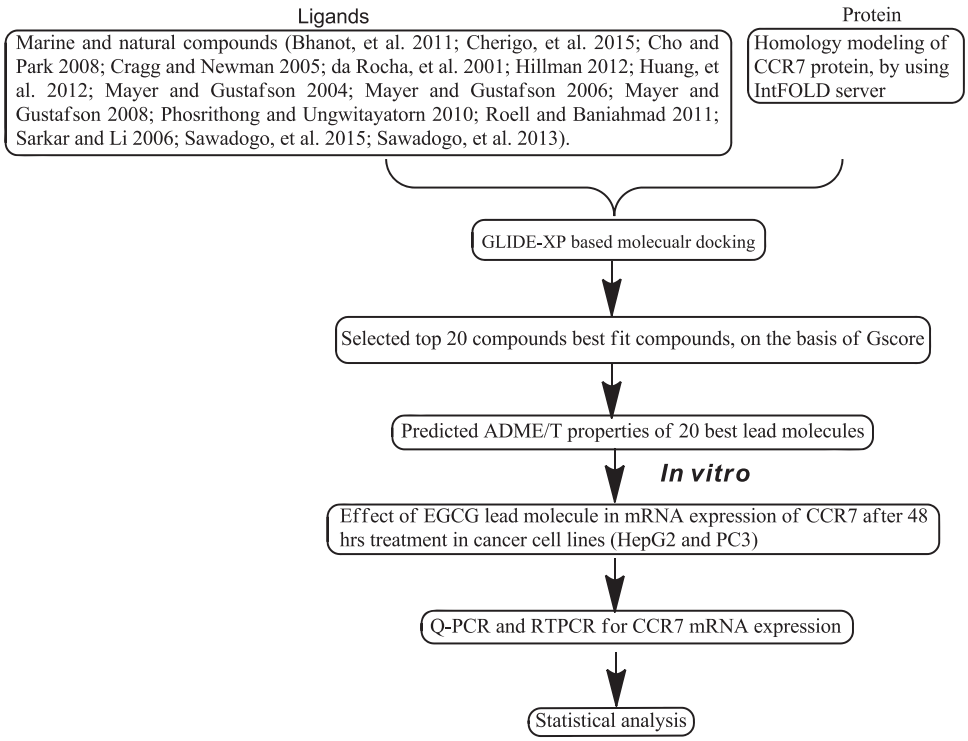

Fig. 1 Workflow of study design

numbered amino acid in the sequence (on the x-axis) (McGuffin, 2008). Figure 2(c) Provide the result of the calculated volumes of atoms in macromolecules using an algorithm which treats the atoms like hard spheres and calculates a statistical *Z*-score deviation for the model from highly resolved (2.0 Å or better) and refined (*R*-factor of 0.2 or better) carried out using structural analysis and verification server (SAVS). Figure 2(d) represents overall quality factor and Ramachandran plot determined by SAVS. Moreover, the model was evaluated by Ramachandran plot provided by procheck and errat plot in SAVS. Predicted structures have the *Z*-score mean, SD, and RMS of −0.197, 1.59, and 1.6 respectively. Furthermore, the overall quality factor of protein structure is 85.62 determined by SAVS.

Molecular docking of model of CCR7 with natural and marine compounds

A natural and marine compound comprises a significant group of structurally diverse low molecular mass molecules. Molecular docking of natural and marine derivatives to the active site of human CCR7 was carried out using GLIDE-XP available with Maestro 9.6. The best-docked compounds have been selected for CCR7 by optimal energy value (Gscore), type of interactions, and conformations. CID6441009, 42607750, 72276, 6711419, 56835050, 65064, 23663412, 72277, 643668, 54679285 compounds have a better binding energy of −11.35, −10.51, −10.16, −9.98, −9.95, −9.86, −9.83, −9.57, −9.47, and −9.45 respectively when selected compounds docked with CCR7. Figure 2 depicts the binding conformations of natural and marine derivatives in the binding pockets of CCR7. Protein—ligand interactions profile highlighted that amino acids Glu45, Lys50, Arg54, Lys57, Trp114, Met260, Glu205, Gln227, Gln276, and Asp309 are involved in the hydrophobic hydrogen bonding and π–π stacking interactions and play a mid role at the active site. (Table 1) Ligand preparation of CID6441009 yielded three isoforms as presented in Table 2. Two isoforms of these compounds have better G score out of twenty best hits. Protein–ligand interactions profile of the CCR7 complex with EGCG highlighted that, the active site of CCR7 comprises of lipophilic, electrostatic, and hydrogen bond interactions. Furthermore, protein–ligand interactions of CCR7 with EGCG depict that amino acids Leu61, Ala118, Trp122, Phe131, Ala207, Met208, and Tyr308 are appeared in the hydrophobic interactions. Moreover, amino acids Tyr65, Glu205, and Asp309, are occupied in side-chain hydrogen bond formation whereas, amino acids Ser117 and Lys120 in backbone hydrogen bonding of interactions (Table 2). Moreover, Trp114 involved in π–π stacking interactions and Lys57 and Arg209 involved in π–cation interaction.

ADME/T properties of leads molecules

An ADME/T property of drug like molecules is a vital aspect to be considered throughout the drug discovery process. Many drugs are incapable to pass clinical trials

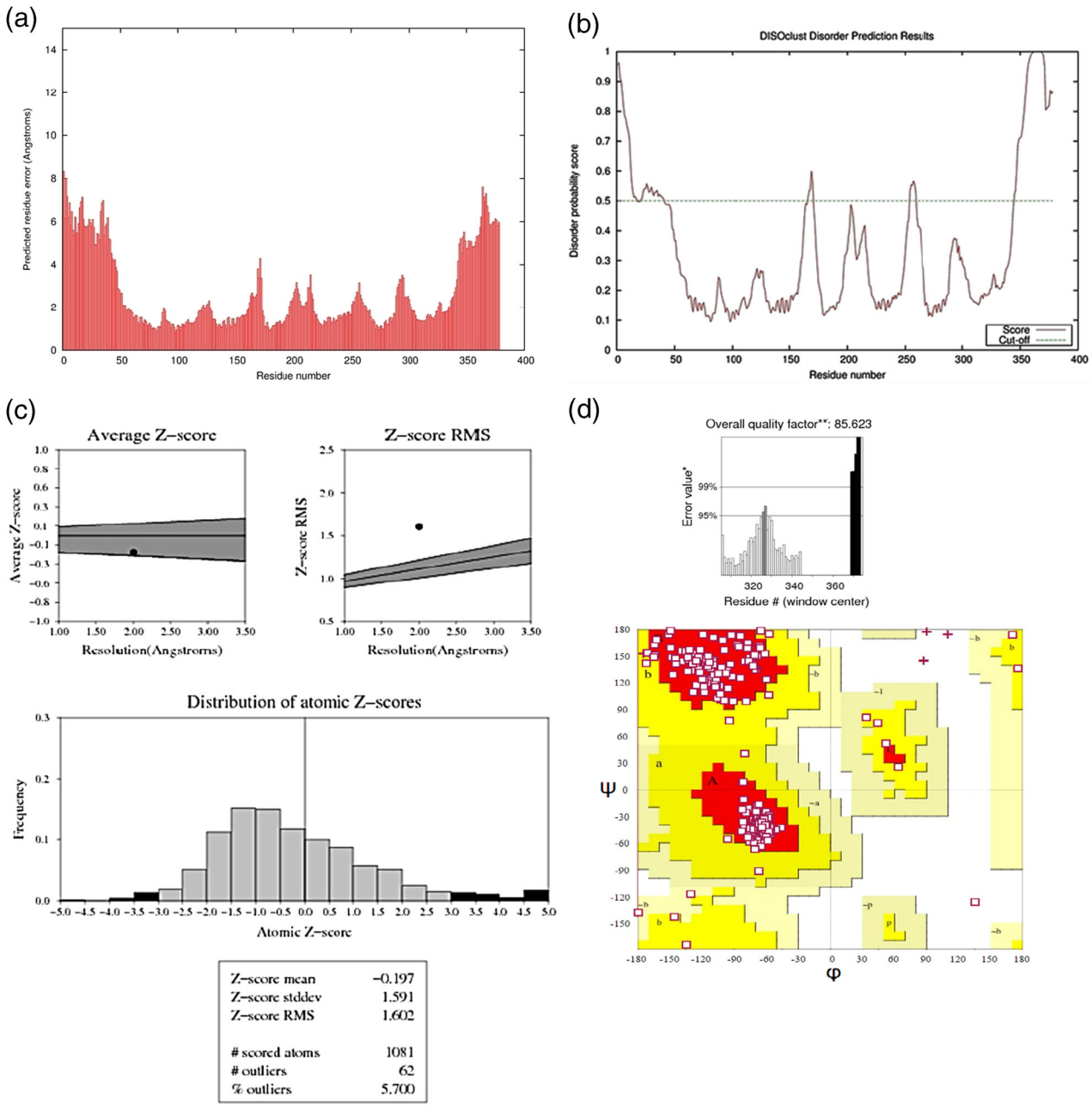

Fig. 2 **a** Model quality assessment is carried out using ModFOLDclust2 and predicted the per-residue error in shown in angstroms. **b** Disorder prediction plot from DISOclust 2.0. The image displays a plot of the probability of disorder (on the y-axis) for each numbered amino acid in the sequence (on the x-axis). **c** Prove results calculates the volumes of atoms in macromolecules using an algorithm which treats the atoms like hard spheres and calculates a statistical *Z*-score deviation for the model from highly resolved (2.0 Å or better) and refined (*R*-factor of 0.2 or better) carried out using structural analysis and verification server (NIH MBI Laboratory Servers). **d** Overall quality factor and Ramachandran plot determined by structural analysis and the verification server

because of their poorer ADME/T profile. Thus, ADME/T properties of lead molecules were evaluated by using the Qikprop application of Maestro 9.6. Compound CID6441009 have good QPlogHerg (−5.132), QPlogBB (−3.965), and QPlog Khsa (−0.44) drug like satisfactory value. Moreover, CID42607750 have a drug like satisfactory value QPlogP, QPlog Herg, QPlogBB, and QPlog Khsa, −0.596, −5.738, −3.387, −0.888 respectively but do not have good percent human oral absorption. Furthermore, CID65064 have good QPlogP, QPlogerg, QPogBB, and QPlog Khsa, −0.512, −5.3, −4.3, and −0.48 value respectively which satisfy the Lipinski's rule of five. ADME properties of lead molecules, such as QPlogPo/w, QplogHerg, QPPCaco, QplogBB, QPPMDCK, QplogKp, Qplog Khsa, and percentage of human oral absorption values are underlined in Tables 3 and 4.

Table 1 List of PubChem molecules screened in this study with structural and physicochemical parameters

S. no.	Comp. (CID)	Mol. wt. (130–725)	Dipole	SASA	Volume (500–2000)	H-bond donor (0–6)	H-bond accp. (2–20)	QPlogS mol/L (−6.5 to 0.5)	CIQPlogS
1	932	272.257	3.889	501.945	840.858	2	4	−3.47	−3.927
2	2543	310.435	1.711	643.151	1122.807	1	1.5	−6.637	−5.657
3	3220	270.241	3.19	479.225	808.031	1	4.25	−3.07	−3.86
4	3712	147.176	2.894	353.487	549.524	2	1.7	−1.606	−1.938
5	4477	327.123	9.701	532.51	895.198	1	3.25	−4.718	−5.269
6	5350	177.279	6.64	428.272	661.845	0	6.5	0.832	0.177
7	9064	290.272	4.628	511.029	872.256	5	5.45	−2.609	−3.474
8	10494	456.707	3.894	694.597	1401.839	2	3.7	−7.067	−6.947
9	16078	314.467	0.973	650.505	1147.852	1	1.5	−6.774	−5.482
10	64945	456.707	3.856	686.213	1387.747	2	3.7	−6.917	−6.947
11	65064	458.378	6.825	696.583	1255.718	8	8.75	−3.547	−5.549
12	68077	372.374	6.233	597.681	1097.414	0	6.25	−3.457	−5.041
13	72276	290.272	2.942	509.472	872.747	5	5.45	−2.587	−3.474
14	72277	306.271	4.452	519.886	892.591	6	6.2	−2.356	−3.446
15	72281	302.283	4.457	541.774	919.955	2	4.75	−3.782	−4.252
16	72326	442.724	1.87	691.613	1393.324	2	3.4	−6.784	−6.65
17	73641	488.706	4.498	699.894	1431.328	4	7.1	−5.37	−6.07
18	73659	472.707	3.881	696.739	1414.592	3	5.4	−6.242	−6.497
19	91469	242.274	2.982	474.852	798.666	2	2.25	−3.579	−3.849
20	94162	300.44	2.934	567.737	1026.407	1	2.75	−5.293	−4.582
21	100308	338.983	2.515	438.812	729.772	2	4.7	−3.547	−5.391
22	107985	360.406	6.257	505.807	991.881	0	9.7	−0.398	−2.045
23	114778	314.424	1.369	496.893	946.696	2	2.95	−3.636	−4.657
24	122724	450.617	7.772	661.025	1317.989	2	4.75	−6.144	−6.869
25	122826	228.25	6.292	431.249	726.321	1	3	−2.787	−3.424
26	124198	332.439	5.815	601.825	1090.725	1	4.5	−5.123	−4.622
27	160254	296.365	6.035	538.125	958.923	0	4.75	−3.928	−3.794
28	189219	283.289	3.001	501.388	858.078	0	5	−3.101	−4.029
29	245005	645.745	2.05	842.565	1768.022	3	16.95	−2.414	−4.706
30	252682	365.357	8.397	530.056	988.252	2	8.25	−2.201	−4.096
31	259846	426.724	1.655	689.205	1378.31	1	1.7	−7.907	−7.136
32	261265	430.626	3.368	720.693	1380.372	2	6.15	−6.081	−5.611
33	362388	190.632	7.884	381.826	602.906	6	4.7	0.351	−0.438
34	403773	286.456	1.625	563.039	1019.646	1	0.75	−5.9	−4.987
35	440917	136.236	0.314	386.657	621.544	0	0	−4.003	−4.286
36	441794	496.553	9.011	672.945	1352.685	5	12.35	−3.295	−4.456
37	442793	294.39	3.582	633.69	1087.774	1	4.2	−4.334	−3.88
38	445154	228.247	2.312	482.188	786.572	3	2.25	−2.803	−3.396
39	446925	536.882	0.565	1267.699	2240.512	0	0	−21.136	−21.136
40	457964	338.486	3.44	542.874	1038.465	4	5.85	−3.013	−3.494
41	2779853	211.192	8.252	382.513	609.005	0	5	−0.764	−1.713
42	5270604	426.724	2.18	686.118	1374.435	1	1.7	−8.012	−7.196
43	5280343	302.24	3.491	531.869	883.724	4	5.25	−3.1	−4.043
44	5280373	284.268	4.292	505.596	860.144	1	3.75	−3.523	−4.447
45	5280443	270.241	4.57	492.818	822.477	2	3.75	−3.377	−4.101
46	5280445	286.24	4.704	503.657	843.558	3	4.5	−3.096	−4.073
47	5280789	538.898	0.65	1272.251	2258.212	0	0	−21.32	−21.32
48	5280863	286.24	3.653	501.189	840.186	3	4.5	−3.057	−4.073

Table 1 continued

S. no.	Comp. (CID)	Mol. wt. (130–725)	Dipole	SASA	Volume (500–2000)	H-bond donor (0–6)	H-bond accp. (2–20)	QPlogS mol/L (−6.5 to 0.5)	CIQPlogS
49	5280896	264.321	3.192	490.169	879.908	2	4.75	−2.772	−2.86
50	5280899	568.881	1.316	1152.469	2125.207	2	3.4	−12.471	−9.573
51	5280961	270.241	4.527	480.83	807.798	2	3.75	−3.014	−4.101
52	5281605	270.241	7.17	489.234	818.653	2	3.75	−3.317	−4.101
53	5281607	254.242	5.656	480.381	799.677	1	3	−3.647	−4.123
54	5281612	300.267	5.118	532.639	901.458	2	4.5	−3.694	−4.429
55	5281614	286.24	6.519	502.899	841.842	4	5.5	−2.796	−3.678
56	5281616	270.241	4.525	488.742	817.396	2	3.75	−3.308	−4.101
57	5281670	302.24	7.116	508.845	858.834	4	5.25	−2.753	−4.043
58	5281672	318.239	4.894	522.847	882.348	5	6	−2.564	−4.011
59	5281707	268.225	4.88	465.198	774.132	2	4.5	−2.915	−3.871
60	5281708	254.242	3.979	470.971	787.865	2	4	−2.957	−3.71
61	5283218	446.539	4.506	782.92	1494.682	0	8	−4.586	−5.08
62	5337997	275.22	7.217	529.502	858.379	2	4.75	−3.252	−3.561
63	5469060	641.545	12.162	807.472	1614.492	1.5	9.25	−3.563	−6.968
64	6400741	664.383	7.247	919.468	1638.505	4	10.9	−6.567	−8.827
65	6436722	542.93	0.634	1265.946	2281.963	0	0	−21.567	−21.567
66	6441009	785.023	9.793	945.341	2125.518	9	21.15	−3.059	−6.052
67	6857485	276.504	0.073	560.026	1033.576	0	0	−9.421	−9.421
68	9548699	274.489	0.17	512.617	963.037	0	0	−8.689	−8.689
69	9548711	278.52	0.112	588.882	1081.565	0	0	−9.074	−9.074
70	9589366	956.233	5.514	914.662	1889.151	5	12.6	−5.405	−14.667
71	9812534	1110.352	10.825	1391.54	3123.119	1.25	27.2	−1.883	−7.047
72	9817550	293.287	8.819	504.622	857.566	5	6.5	−2.922	−3.611
73	9892144	499.476	2.785	732.249	1372.61	3	7	−5.902	−8.029
74	10041259	313.315	9.802	534.201	930.847	0	7	−2.675	−3.739
75	10373128	793.953	12.399	1326.976	2497.984	8.25	19.95	−7.114	−6.357
76	11210478	356.221	2.816	603.722	1024.595	1	5	−5.837	−6.176
77	11273547	616.879	5.839	1144.065	2155.891	2	7.15	−10.652	−8.734
78	11721258	587.633	4.886	820.741	1675.24	2	6.4	−7.674	−8.707
79	11724205	330.466	4.392	586.228	1087.014	1	3.5	−5.2	−4.907
80	11808929	306.317	2.629	538.764	940.256	0	5.75	−3.253	−3.796
81	16737543	438.611	2.063	739.628	1384.199	0	4.25	−6.626	−6.329
82	44558968	436.676	4.461	1092.923	1847.468	3	3.4	−10.412	−6.482
83	54679285	412.525	6.541	794.608	1424.61	1	4.75	−7.03	−6.541
84	985	256.428	2.296	678.27	1131.975	1	2	−5.637	−3.576
85	3365	306.274	7.604	470.201	850.243	1	6.75	−1.844	−3.74
86	6253	243.219	3.507	431.03	723.357	5	10.8	−1.509	−1.035
87	6300	300.44	5.819	537.065	990.95	1	2.75	−4.775	−4.438
88	7020	196.205	2.978	403.949	655.353	0	2.5	−2.904	−2.919
89	11379	144.176	2.799	345.174	534.532	2	1.5	−1.632	−1.987
90	25051	225.204	8.3	409.131	674.99	3	8.1	−1.301	−1.469
91	28620	943.09	11.883	1261.404	2567.723	9	30.95	−4.728	−5.602
92	44259	466.538	7.904	673.38	1290.069	2	6.45	−4.606	−6.358
93	71734	565.792	7.601	1179.183	2084.975	4	12.8	−8.354	−5.838
94	72495	627.965	2.63	1076.035	2047.626	6	9.7	−5.243	−4.375
95	73431	638.581	3.573	887.324	1706.716	2	11.9	−6.429	−8.509
96	100308	338.983	2.515	438.812	729.772	2	4.7	−3.547	−5.391

Table 1 continued

S. no.	Comp. (CID)	Mol. wt. (130–725)	Dipole	SASA	Volume (500–2000)	H-bond donor (0–6)	H-bond accp. (2–20)	QPlogS mol/L (−6.5 to 0.5)	CIQPlogS
97	107713	579.692	2.14	850.705	1724.808	1	11.65	−4.851	−5.536
98	108150	761.842	6.012	858.09	1863.922	4	16.2	−1.528	−6.009
99	122838	318.328	6.129	523.594	933.037	0	6.5	−2.736	−3.758
100	178028	640.865	3.489	966.393	1989.658	1.25	15.25	−1.48	−2.019
101	222284	414.713	2.033	770.779	1471.748	1	1.7	−8.613	−7.033
102	223997	300.397	6.607	518.421	957.915	0	6	−2.9	−2.911
103	339816	346.422	1.461	552.972	1039.164	0	8	−2.019	−3.085
104	340129	320.471	5.07	595.683	1093.989	1	4	−4.867	−4.269
105	354399	985.228	16.265	1131.921	2668.233	0.75	22	1.14	−5.345
106	439260	169.18	3.3	366.985	585.996	5	4.2	0.674	−0.361
107	443237	410.682	2.251	740.721	1426.622	1	1.7	−8.215	−7.078
108	636710	732.999	8.435	1025.654	2231.813	1.25	16.85	−1.898	−4.627
109	636718	665.6	5.919	902.589	1778.609	1	11.75	−5.988	−8.585
110	636888	280.32	3.265	556.727	943.897	3	7.55	−2.818	−2.451
111	636989	599.744	5.934	798.916	1697.192	1	13.5	−1.112	−4.631
112	637018	332.439	4.494	551.293	1027.106	1	6.15	−3.995	−3.355
113	637424	428.611	4.692	662.748	1313.182	1	4.2	−6.483	−6.304
114	637473	220.354	1.581	473.118	831.967	1	1.7	−3.925	−3.028
115	639674	448.685	4.903	754.483	1489.776	2	7.4	−5.758	−5.202
116	643668	593.799	10.409	1029.433	1990.276	6	12.3	−6.545	−6.087
117	643725	439.55	5.08	780.38	1449.593	3	6.95	−6.238	−5.209
118	2826713	858.333	12.136	1796.842	3274.889	7	16.1	−12.437	−9.003
119	5280794	412.698	2.064	755.687	1452.374	1	1.7	−8.494	−6.991
120	5280953	212.251	2.978	444.923	731.607	1	1.75	−3.561	−3.544
121	5281328	412.698	1.981	766.84	1463.14	1	1.7	−8.702	−6.991
122	5311436	374.433	1.228	714.132	1313.906	0	7	−4.62	−3.778
123	5324375	318.215	1.808	543.377	918.67	1	3	−3.723	−4.196
124	5324595	276.254	9.365	430.491	749.464	3	4.5	−2.624	−4.065
125	5352092	526.718	4.148	854.936	1699.82	2.25	8.25	−5.468	−4.755
126	5372499	154.165	3.082	374.339	579.955	2	5.4	−1.231	−0.816
127	5386394	325.121	10.371	458.544	769.253	4	7	−2.884	−3.433
128	5471086	456.664	4.27	929.958	1691.779	0	5.7	−8.576	−6.357
129	5472714	332.439	5.398	567.043	1081.218	0	7	−3.135	−2.473
130	5481589	545.545	4.173	785.115	1498.814	2	7.75	−6.49	−8.633
131	5488895	1111.328	3.621	1334.033	2927.693	3	25.2	−7.438	−12.031
132	6326668	840.129	4.08	1091.124	2420.913	1.25	16.7	−4.951	−8.104
133	6439795	321.421	4.763	627.168	1104.585	2	2.25	−6.139	−5.566
134	6440837	358.477	1.784	678.982	1226.842	1	5.5	−5.473	−4.765
135	6445533	379.458	8.703	698.597	1244.504	4	7.9	−2.8	−3.515
136	6473739	905.044	4.204	1274.3	2634.198	3	17.1	−8.297	−10.783
137	6711419	517.615	10.024	769.373	1539.209	3	15.9	−2.057	−2.983
138	6918335	656.772	11.346	994.922	1962.576	2	14.3	−6.859	−7.208
139	6918506	548.67	3.903	811.94	1643.514	5	15.4	−3.818	−3.544
140	6918637	473.654	2.227	783.545	1554.738	2.25	8.25	−4.296	−3.512
141	9794358	213.233	6.602	409.763	695.068	0.25	6.45	0.569	−0.274
142	9796387	301.255	3.9	523.873	893.285	2	8.95	−1.2	−1.605
143	9810929	785.096	10.15	1198.449	2463.328	1.25	17.15	−4.432	−5.221
144	9812534	1110.352	8.767	1220.975	2957.143	1.25	27.2	0.764	−7.047

Table 1 continued

S. no.	Comp. (CID)	Mol. wt. (130–725)	Dipole	SASA	Volume (500–2000)	H-bond donor (0–6)	H-bond accp. (2–20)	QPlogS mol/L (−6.5 to 0.5)	CIQPlogS
145	9814817	299.496	2.689	719.615	1232.063	3	4.4	−3.742	−2.391
146	9831636	709.679	8.108	882.897	1871.011	2.25	9	−4.605	−8.949
147	9892144	499.476	2.785	732.249	1372.61	3	7	−5.902	−8.029
148	9918978	837.067	8.937	1162.861	2480.358	0.25	18.5	−3.775	−5.553
149	9925886	285.512	2.007	741.492	1269.347	3	2.7	−4.293	−2.619
150	9929833	381.474	4.655	704.462	1256.672	2	6.25	−4.197	−3.905
151	9949641	336.393	6.047	631.518	1101.58	3	6.5	−4.544	−4.424
152	10017010	288.472	2.402	509.009	1001.779	1	1.7	−4.742	−4.061
153	10045316	380.302	6.744	589.258	1031.771	2	4.25	−3.734	−4.885
154	10053416	555.774	1.76	948.59	1837.36	1	7.5	−4.967	−5.726
155	10258174	610.654	12.17	777.977	1640.645	2	16.4	−3.247	−4.652
156	11069750	416.513	9.158	695.464	1327.634	0	7	−5.243	−4.453
157	11181528	687.829	4.331	1142.563	2175.674	2	15.35	−5.622	−5.622
158	11300750	290.315	4.826	512.903	913.408	0	6.7	−2.266	−2.401
159	11346628	283.754	8.784	511.648	889.057	1	6.7	−3.306	−2.63
160	11347535	313.78	8.147	527.749	940.785	0.25	6.45	−1.666	−2.391
161	11349752	388.503	3.1	708.7	1337.862	0	6	−4.389	−4.775
162	11354606	729.906	3.075	910.421	1954.404	3	18.1	−2.08	−5.994
163	11751733	469.129	5.154	673.043	1147.402	3	4.75	−5.836	−7.364
164	11783867	381.898	2.705	575.927	1091.042	1	5.75	−4.998	−4.916
165	11784261	396.612	5.395	734	1368.097	1	3.7	−7.477	−5.914
166	11972518	1111.328	3.712	1356.53	2967.073	3	25.2	−7.81	−12.031
167	14161394	428.697	0.95	768.698	1477.08	2	2.45	−7.846	−6.874
168	16075395	512.383	6.055	737.89	1328.728	9	8.75	−3.444	−6.856
169	21589702	534.732	6.649	854.311	1686.233	3	9.1	−6.653	−6.36
170	21773232	562.742	5.819	825.971	1757.31	2	9.85	−3.525	−6.521
171	24867082	654.756	9.534	1058.13	2044.742	1	13	−6.381	−7.27
172	42607750	462.409	10.521	708.183	1281.697	6	14	−2.784	−3.918
173	44299148	466.538	7.904	673.38	1290.069	2	6.45	−4.606	−6.358
174	44448144	1163.553	6.332	1364.436	3066.15	6	16.35	−8.508	−11.831
175	44584763	612.67	8.763	760.878	1632.03	3	14.2	−3.762	−5.682
176	44584773	312.448	2.107	617.883	1129.599	1	4.45	−4.286	−4.018
177	50901240	840.068	7.039	1078.044	2401.63	1.5	18.2	−2.572	−5.969
178	53355697	377.442	6.307	675.498	1212.8	1	7	−4.23	−4.279
179	56835050	743.046	3.547	1055.551	2182.748	4	14.8	−6.33	−8.14
180	56841540	1367.422	19.957	1366.866	3249.463	8	41.4	0.879	−9.058
181	56928089	1110.352	7.724	1122.642	2847.601	1.25	27.2	2	−7.047
182	60155155	896.094	10.112	1175.474	2553.449	2.75	18.75	−3.543	−6.325
183	70683403	386.53	3.955	788.875	1406.458	1	3.5	−7.585	−6.139
184	70690672	1013.655	11.911	1246.12	2750.981	6	21.35	−5.849	−11.089
185	70694527	312.327	1.991	547.606	949.629	5	5.75	−2.717	−2.855
186	78357789	717.988	9.77	1119.233	2303.026	3.25	16.85	−3.171	−3.662

Compounds; PubChem molecules screened in this study

Molecular weight (<500 Da)

Volume; Estimated number of hydrogen bonds that would be accepted by the solute from water molecules in an aqueous solution. Values are averages taken over a number of configurations, so they can be non-integer

Hydrogen bond donors (<5)

Hydrogen bond acceptors (<10)

QPlog S; was Predicted aqueous solubility; S in mol/L (acceptable range: −6.5–0.5)

Table 2 Lowest binding energy for the ligand (Control)-CCR7 interaction as detected by GLIDE molecular docking

S.N.	Ligand (CID)	GScore	Lip	H-Bond	Electro	Protein–ligands interactions
1	3009355	−7.86	−2.76	−1.2	−0.7	Glu45, Lys50, Arg54, and Gln286
2	3001322	−7.74	−3.17	−2.22	−1.32	Lys137 and Gln276
3	3002977	−7.38	−3.42	−0.47	−0.93	Lys137, Arg209, Tyr79, and Tyr312

Table 3 Lowest binding energy for the ligand-CCR7 protein interaction as detected by GLIDE molecular docking

S.N.	Ligands (CID)	GScore	Lip	H-bond	Electro	Protein–ligands interactions
1	6441009	−11.35	−3.31	−4.25	−1.3	Glu45, Lys50, Arg54, Glu193, and Gln286
2	42607750	−10.51	−4.4	−3.4	−0.71	Lys137, Arg209, and Gln276
3	72276	−10.16	−2.9	−2.01	−1.14	Lys137, Arg209, Tyr79, and Tyr312
4	6711419	−9.98	−2.56	−4.25	−1.46	Lys57, Tyr65, Sre117, Met260, and Tyr312
5	56835050	−9.95	−4.8	−2.93	−1.2	Leu47, Lys137, Gln227, and Tyr308
6	65064	−9.86	−3.04	−4.62	−1.73	Lys57, Trp114, Met260, Glu205 and Asp309
7	23663412	−9.83	−3.55	−2.94	−1.86	Lys57, Lys137, and Arg209
8	72277	−9.57	−2.99	−3.18	−0.68	Lys137 and Gln227
9	643668	−9.47	−4.69	−2.09	−0.97	Glu45, Lys137, and Asn305
10	54679285	−9.45	−4.95	−1.23	−0.29	Phe140, Cys210, and Lys137, Gln227
11	42607750-2	−9.38	−3.43	−2.95	−0.68	Glu45, Tyr136, Phe140, and Tyr312
12	73431	−9.3	−3.74	−3.54	−0.81	Glu45, Lys137, and Arg209
13	54679285-2	−9.28	−4.96	−1.09	−0.15	Phe140, Leu212, and Gln276
14	6441009-2	−9.18	−3.36	−3.54	−0.58	Arg209 and Asp309
15	54679285-3	−8.96	−4.42	−1.27	−0.27	Cys210 and Gln276
16	54679285-4	−8.93	−4.13	−1.35	−0.67	Lys137, Phe140, Gln276 and Asp309
17	6436722	−8.85	−6.96	0	−0.01	
18	54679285-5	−8.81	−4.5	−0.94	−0.19	Phe140, Leu212, and Gln276
19	54679285-6	−8.71	−3.54	−1.79	−0.61	Lys50, Lys137, Phe140, and Gln276
20	6711419-2	−8.67	−4.1	−2.49	−0.5	Tyr136, Lys137, Gln227, and Gln276

Ligand CID Pubchem IDs, *GScore* Glide extra precision scores (kcal/mol), *Lipophilic E Vdw* chemscore lipophilic pair term and fraction of the total protein–ligand vdw energy, *H-bond* Hydrogen bonding term, *Electro*, electrostatic rewards, *Protein–ligands interaction* π–π stacking, π–cat interaction and hydrogen bond between the ligands and protein

Effect of EGCG on CCR7 mRNA expression in cancer cell lines

We investigated whether EGCG could impede CCR7 expression in HepG2 and PC3 cells. After 48 h of treatment with EGCG, the mRNA expression was determined in cells by using semiquantitative and quantitative real-time PCR using GAPDH as a control (Fig. 3). As shown in Fig. 4(a), Q-PCR showed that EGCG down-regulated the expression of CCR7 mRNA in HepG2 (30 %) and in PC3 (10 %). Moreover, Fig. 4(b) RT-PCR demonstrates that EGCG have a potential for robust inhibition of CCR7 mRNA. Previous reports from our lab show that EGCG reduce cell proliferation and ROS generation after 48 h treatment in HepG2, and PC3 human cell lines. Interestingly, our result also indicates that reduction in potential for colony formation and cell migration enhances the anti-metastasis activity of EGCG (Singh and Bast, 2015a, c).

EGCG diminishes chemokine production by inhibiting the production of IL-8 and MIP-3α in TNFα stimulated colon epithelial (T84) cells that leads to the down-regulation of genes involved in inflammatory pathways (Porath et al., 2005). Moreover, EGCG has been shown to inhibit inflammatory signaling pathways via regulating pro-inflammatory mediators' such as the reduction of nuclear factor-$\kappa\beta$ and activator protein-1 (Abboud et al., 2008). In recent years, natural polyphenols, marine compounds, and their synthetic analogs have been investigated intensely in the treatment of ovarian, breast, cervical, pancreatic, and prostate cancers. Many promising new agents are in clinical development based on discriminatory activity against anticancer molecular targets. Natural compounds such as quercetin, genistein or flavopiridol (a synthetic analog of a natural alkaloid Rohitukin) have entered the late phase clinical trials accredited to their oncological indications with the conspicuous absence of recognizable side effects. At the

Table 4 ADME/T properties of lead compounds were appraised by using the Qikprop application of Maestro 9.6

S.N.	Ligand (CID)	QP log $P_{o/w}$ (−2.0 to 6.5)	QP log Herg (acceptable range: above −5.0)	QPP Caco (nm/s) <25—poor; >500—great	QP log BB (−3 to 1.2)	QPP MDCK (nm/s) <25—poor; >500—great	QPlog Khsa (acceptable range: −1.5 to 1.5)	Percent human oral absorption >80 %—high; <25 %—poor
1	6441009	1.351	−5.132	11.756	−3.965	4.06	−0.446	15.139
2	42607750	−0.596	−5.738	11.061	−3.387	3.801	−0.888	16.222
3	72276	0.273	−4.41	48.035	−1.856	18.589	−0.453	58.642
4	6711419	0.911	−3.587	604.119	−1.186	520.97	−1.029	56.138
5	56835050	5.767	−3.072	22.788	−2.918	62.379	0.264	46.135
6	65064	−0.512	−5.385	0.785	−4.321	0.218	−0.481	0
7	23663412	3.509	−4.674	18.752	−3.843	8.554	−0.553	44.36
8	72277	−0.382	−4.167	19.239	−2.255	6.915	−0.588	34.732
9	643668	4.054	−5.822	44.818	−3.545	17.247	0.387	54.322
10	54679285	5.763	−6.294	973.648	−1.352	480.634	1.047	100
11	42607750	−0.555	−5.587	14.664	−3.199	5.156	−0.89	18.653
12	73431	3.06	−6.252	10.772	−3.624	3.694	0.513	24.464
13	54679285	5.762	−6.332	1015.569	−1.329	503.04	1.036	100
14	6441009	1.353	−5.143	14.147	−3.875	4.959	−0.468	16.587
15	54679285-3	5.219	−6.137	1500.639	−1.046	767.156	0.634	100
16	54679285-4	5.811	−6.283	1046.255	−1.313	519.488	1.059	100
17	6436722	18.413	−7.437	9906.038	2.412	5899.293	4.2	100
18	54679285-5	5.231	−6.232	1236.169	−1.155	622.122	0.664	100
19	54679285-6	5.158	−5.832	1966.678	−0.876	1027.64	0.572	100
20	6711419-2	0.937	−3.492	605.677	−1.171	518.205	−1.012	56.312

Ligand (CID) Pubchem IDs of the lead molecules, *QPog*$P_{o/w}$ *(−2.0 to 6.5)* predicted octanol/water partition coefficient log *P* (range: −0.20 to 6.5) [Predicted IC_{50} values for blockage of Herg K^+ channels; (acceptable range: above −5.0)],

QPP Caco predicted apparent Caco-2 cell permeability in nm/s [Caco-2 cells is a model for the gut blood barrier; (nm/s) <25—poor >500—great],

QPlog BB predicted brain/blood partition coefficient, *QPP MDCK* predicted apparent MDCK cell permeability in nm/s [MDCK cells are considered to be a good mimic for the blood-brain barrier; (nm/s) <25—poor; >500—great], *QPlog* K_{hsa} prediction of binding to human serum albumin (acceptable range: −1.5 to 1.5) [Percentage of human oral absorption; (<25 % is poor and >80 % is high)]

molecular level, natural polyphenols and marine compounds have been reported to modulate diverse protein kinases including receptor tyrosine kinases (RTKs) and modulating enzymes activity such as xanthine cyclooxygenase and lipoxygenase which play a significant role in cancer pathology (Liu et al., 2012). Due to the complication of the chemokine system in regulating various biological processes, progress of therapeutic agents targeting this system remains quite challenging. Recently forty compounds have been reported to antagonize binding that leads to inhibition of chemokine signaling (Yuan, 2014). Bioactive natural and marine compounds have been found to be indispensable for the growth and development of plants, additionally providing the natural environment that proves to be essential for plant survival under stress condition. The various natural polyphenols and marine compounds have attracted more attention owing to their remarkable spectrum of pharmacological activities such as antioxidant, anti-angiogenic, antiinflammatory, and anticancer activity. Due to their multiple molecular mechanisms of action, the natural polyphenols, and marine compounds are being investigated for their potential applications in anticancer therapies. Natural and marine compounds modulate a variety of biological activities associated with cancer progression and development including the cell proliferation, apoptosis, cell differentiation and neovascularization (Koehn and Carter, 2005). In vitro and in vivo studies have established an irrefutable association between natural and marine compounds induced modulation of protein kinase and matrix metalloproteinases (MMPs) activities with apoptosis, cellular proliferation, tumor cell invasive and inhibition of angiogenesis (Senthilkumar K et al., 2013). Natural and marine compound derivatives have been the most productive source of chemotherapeutic agents but

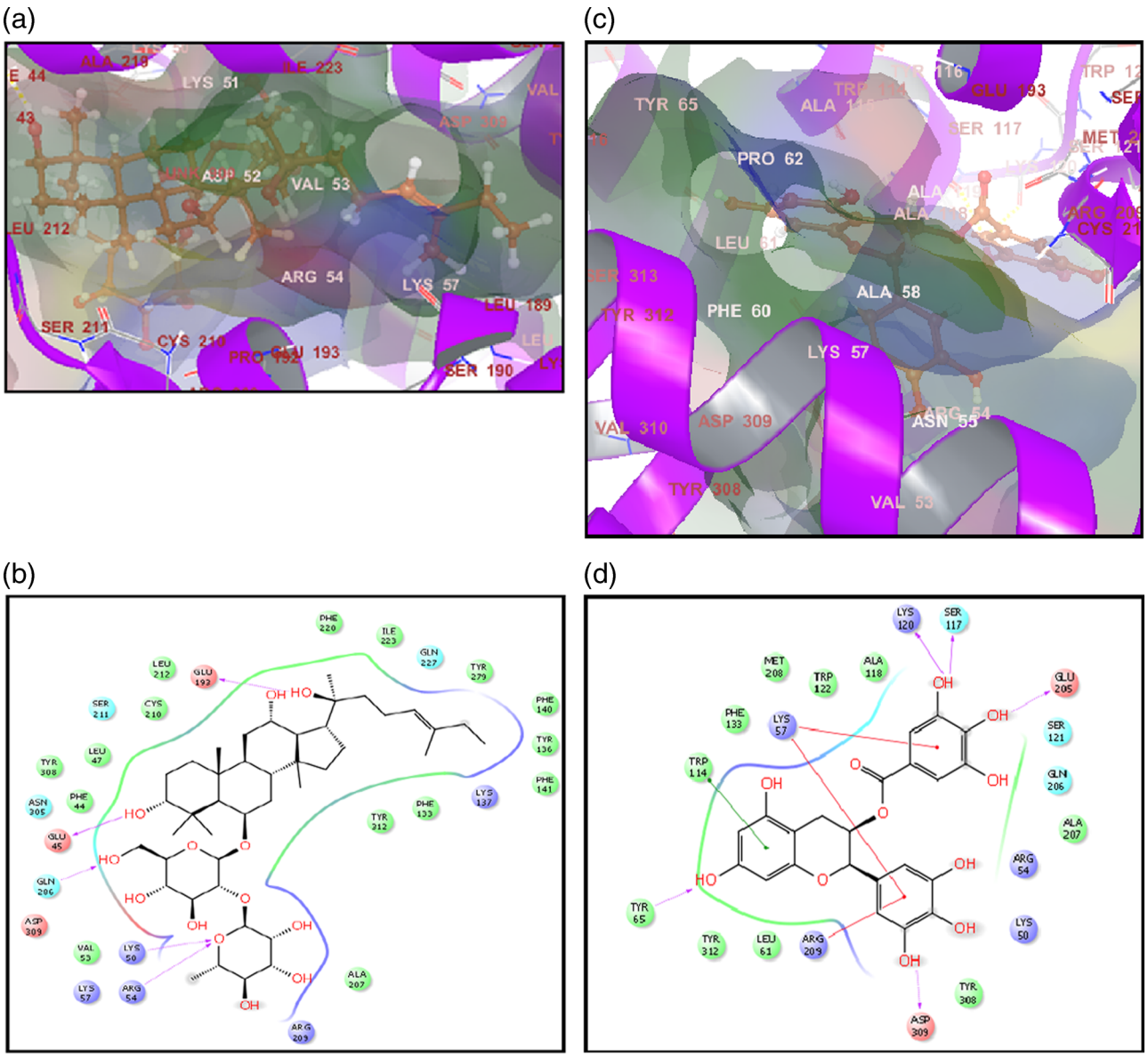

Fig. 3 **a** Ribbon presentation of the CCR7 protein molecule with CID6441009 **b** Protein–ligand interactions profile of CCR7 with CID6441009. **c** Ribbon presentation of the CCR7 protein molecule with CID65064 **d** Protein-ligand interactions profile of CCR7 with CID65064

certain disadvantages, such as low bioavailability and week potency, are the critical pitfall for translating fundamental discoveries into successful clinical trials. Therefore, promotion of natural polyphenyl and marine compounds for anticancer In vitro and In vivo experiment provide the better strategy to understand the mechanism of action of cancer.

Conclusion

CCR7 promoted cancer progression by generating new lymphatic vessels that serve as the channel for tumor dissemination to lymph nodes. Our results showed that CID6441009, 42607750, 72276, 6711419, 56835050, 65064, 23663412, 72277, 643668, 54679285 compound have a superior binding energy −11.35, −10.51, −10.16, −9.98, −9.95, −9.86, −9.83, −9.57, −9.47, and −9.45 respectively against CCR7. Protein–ligand interactions profile accentuated that amino acid Glu45, Lys50, Arg54, Lys57, Trp114, Met260, Glu205, Gln227, Gln276, and Asp309 involved in the lipophilic, hydrogen bonding, π–π stacking, and π-cation interactions play a predominant role at the active site. Foremost, ADME properties of lead molecules, such as QPlogPo/w, QplogHerg, QPPCaco, QplogBB, QPPMDCK, QplogKp, Qplog Khsa, and percentage of human oral absorption values are charted.

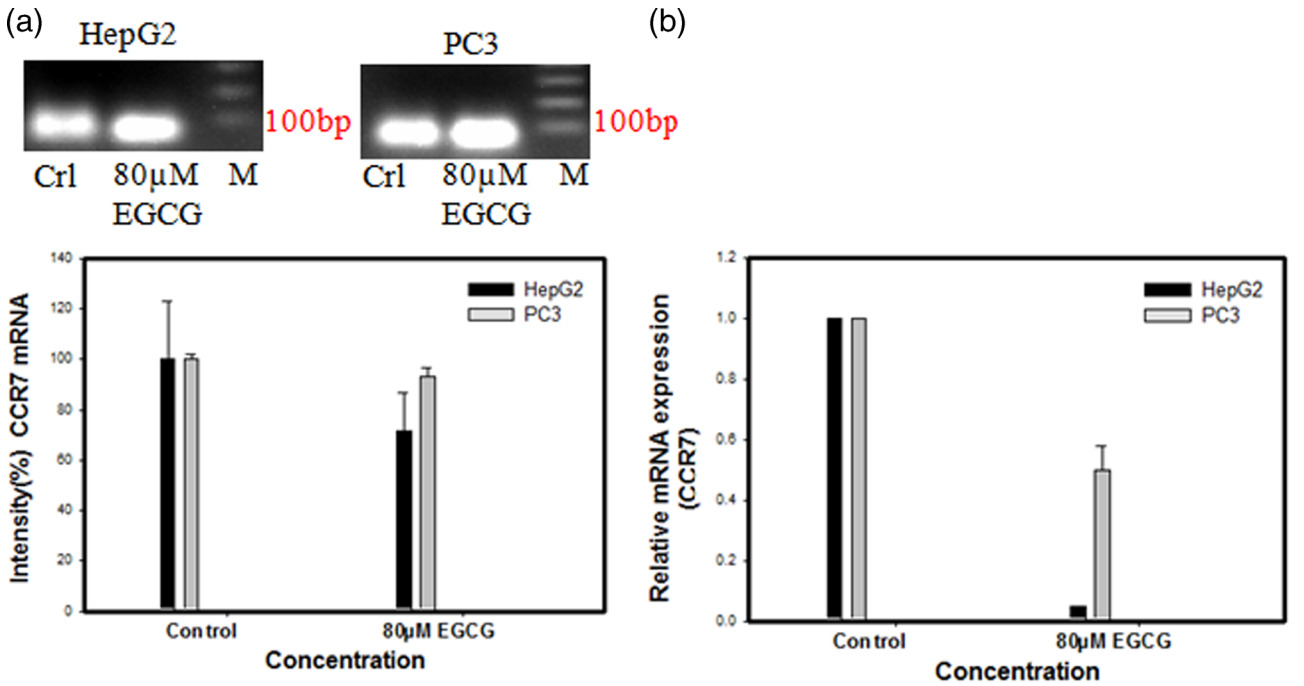

Fig. 4 Figure represented effect of EGCG on CCR7 mRNA turnover in HepG2 and PC3. Cells were treated with 80 μM EGCG for the indicated time periods. **a** CCR7 mRNA levels were determined by Q-PCR and GAPDH used as the loading control. **b** CCR7 mRNA levels were determined by SYBR® Green based RT-PCR. EGCG down-regulated the expression of CCR7 mRNA in HepG2 and PC3

Moreover, treatment with the EGCG led to down-regulation of mRNA expression of CCR7. Inhibition of CCR7/CCL19 signaling axis may provide an auspicious approach for the anti-tumor therapy. This molecular docking study outlined docking free energy, protein–ligands interaction profile, pharmacokinetic, and the pharmacodynamic parameters of lead molecules, which are tremendously helpful to ameliorate the activity of natural and marine compounds against CCR7.

Acknowledgments We would like to thank Vice Chancellor, Central University of Punjab, Bathinda, Punjab, (India) for supporting this study with infrastructural requirements. We also thank Professor P. Ramarao (Dean, Academic Affairs), Central University of Punjab, Bathinda, Punjab, India, for his suggestions during the course that tremendously helped to improve this article. This study was also supported by a Senior Research Fellowship Grant-in-Aid from Indian Council of Medical Research (ICMR), Government of India awarded to PS and RS Singh.

Compliance with ethical standards

Conflict of interest The authors declare that they have no conflict of interest.

References

Abboud PA, Hake PW, Burroughs TJ, Odoms K, O'Connor M, Mangeshkar P, Wong HR, Zingarelli B (2008) Therapeutic effect of epigallocatechin-3-gallate in a mouse model of colitis. Eur J pharmacol 579:411–417

Adams JL, Smothers J, Srinivasan R, Hoos A (2015) Big opportunities for small molecules in immuno-oncology. Nat Rev Drug Discov 14:603–622

Bhanot A, Sharma R, Noolvi MN (2011) Natural sources as potential anti-cancer agents: a review. Int J Phytomed 3:9–26

Biswas S, Criswell TL, Wang SE, Arteaga CL (2006) Inhibition of transforming growth factor-β signaling in human cancer: targeting a tumor suppressor network as a therapeutic strategy. Clin Cancer Res 12:4142–4146

Cherigo L, Lopez D, Martinez-Luis S (2015) Marine natural products as breast cancer resistance protein inhibitors. Marine Drugs 13:2010–2029

Chen, Y., Tian, Y., Ji, Z., Liu, Z., Shang, D. (2015). CC-chemokine receptor 7 is overexpressed and correlates with growth and metastasis in prostate cancer. Tumor Biol 1-5.

Cho JY, Park J (2008) Contribution of natural inhibitors to the understanding of the PI3K/PDK1/PKB pathway in the insulin-mediated intracellular signaling cascade. Int J Mol Sci 9:2217–2230

Cragg GM, Newman DJ (2005) Plants as a source of anti-cancer agents. J Ethnopharmacol 100:72–79

Cunningham HD, Shannon LA, Calloway PA, Fassold BC, Dunwiddie I, Vielhauer G, Zhang M, Vines CM (2010) Expression of the CC chemokine receptor 7 mediates metastasis of breast cancer to the lymph nodes in mice. Transl Oncol 3:354–361

Da Rocha AB, Lopes RM, Schwartsmann G (2001) Natural products in anticancer therapy. Curr Opin Pharmacol 1:364–369

Debnath B, Xu S, Grande F, Garofalo A, Neamati N (2013) Small molecule inhibitors of CXCR4. Theranostics 3:47–75

Ding Y, Shimada Y, Maeda M, Kawabe A, Kaganoi J, Komoto I, Hashimoto Y, Miyake M, Hashida H, Imamura M (2003) Association of CC chemokine receptor 7 with lymph node metastasis of esophageal squamous cell carcinoma. Clin Cancer Res 9:3406–3412

Friesner RA, Banks JL, Murphy RB, Halgren TA, Klicic JJ, Mainz DT, Repasky MP, Knoll EH, Shelley M, Perry JK (2004) Glide: a new approach for rapid, accurate docking and scoring. 1. Method and assessment of docking accuracy. J Med Chem 47:1739–1749

Friesner RA, Murphy RB, Repasky MP, Frye LL, Greenwood JR, Halgren TA, Sanschagrin PC, Mainz DT (2006) Extra precision glide: docking and scoring incorporating a model of hydrophobic enclosure for protein-ligand complexes. J Med Chem 49:6177–6196

Gray AL, Stephens CA, Bigelow RL, Coleman DT, Cardelli JA (2014) The Polyphenols (−)-epigallocatechin-3-gallate and luteolin synergistically inhibit TGF-β-induced myofibroblast phenotypes through RhoA and ERK inhibition. PloS one 9(10): e109208

Halgren TA, Murphy RB, Friesner RA, Beard HS, Frye LL, Pollard WT, Banks JL (2004) Glide: a new approach for rapid, accurate docking and scoring. 2. Enrichment factors in database screening. J Med Chem 47:1750–1759

Hayashi K, Takai S, Matsushima-Nishiwaki R, Hanai Y, Kato K, Tokuda H, Kozawa O (2008) (−)-Epigallocatechin gallate reduces transforming growth factor β-stimulated HSP27 induction through the suppression of stress-activated protein kinase/c-Jun N-terminal kinase in osteoblasts. Life Sci 82:1012–1017

Hillman GG (2012) Dietary agents in cancer chemoprevention and treatment. J Oncol doi: 10.1155/2012/749310. [Epub 18 Dec 2012]

Huang W, He T, Chai C, Yang Y, Zheng Y, Zhou P, Qiao X, Zhang B, Liu Z, Wang J (2012) Triptolide inhibits the proliferation of prostate cancer cells and down-regulates SUMO-specific protease 1 expression. PLoS One 7:e37693

Jorgensen WL, Duffy EM (2002) Prediction of drug solubility from structure. Adv Drug Deliv Rev 54:355–366

Jorgensen WL, Maxwell DS, Tirado-Rives J (1996) Development and testing of the OPLS all-atom force field on conformational energetics and properties of organic liquids. J Am Chem Soc 118:11225–11236

Jorgensen WL, Tirado-Rives J (1988) The OPLS [optimized potentials for liquid simulations] potential functions for proteins, energy minimizations for crystals of cyclic peptides and crambin. J Am Chem Soc 110:1657–1666

Koehn FE, Carter GT (2005) The evolving role of natural products in drug discovery. Nat Revi Drug Discov 4:206–220

Liu L-C, Tsao TC-Y, Hsu S-R, Wang H-C, Tsai T-C, Kao J-Y, Way T-D (2012) EGCG inhibits transforming growth factor-β-mediated epithelial-to-mesenchymal transition via the inhibition of Smad2 and Erk1/2 signaling pathways in nonsmall cell lung cancer cells. J Agr Food Chem 60:9863–9873

Lu JJ, Crimin K, Goodwin JT, Crivori P, Orrenius C, Xing L, Tandler PJ, Vidmar TJ, Amore BM, Wilson AG (2004) Influence of molecular flexibility and polar surface area metrics on oral bioavailability in the rat. J Med Chem 47:6104–6107

Martin S, Pommier Y, Caplen N (2007) RNAi screening identifies TAK1 as a potential target for the enhanced efficacy of traditional cytotoxic agents in breast cancer cells. Mol Cancer Ther 6(11 Suppl):PR-3-PR-3.

Martin S, Wu Z-H, Gehlhaus K, Jones T, Zhang Y-W, Guha R, Miyamoto S, Pommier Y, Caplen N (2011) RNAi screening identifies TAK1 as a potential target for the enhanced efficacy of topoisomerase inhibitors. Curr Cancer Drug Targets 11:976

Mashino K, Sadanaga N, Yamaguchi H, Tanaka F, Ohta M, Shibuta K, Inoue H, Mori M (2002) Expression of chemokine receptor CCR7 is associated with lymph node metastasis of gastric carcinoma. Cancer Res 62:2937–2941

Mayer AM, Gustafson KR (2004) Marine pharmacology in 2001–2: antitumour and cytotoxic compounds. Eur J Cancer 40:2676–2704

Mayer AM, Gustafson KR (2006) Marine pharmacology in 2003–2004: anti-tumour and cytotoxic compounds. Eur J Cancer 42:2241–2270

Mayer AM, Gustafson KR (2008) Marine pharmacology in 2005–2006: Antitumour and cytotoxic compounds. Eur J Cancer 44:2357–2387

McGuffin LJ (2008) Intrinsic disorder prediction from the analysis of multiple protein fold recognition models. Bioinformatics 24:1798–804

Mo M, Zhou M, Wang L, Qi L, Zhou K, Liu L-F, Zu X-B (2015) CCL21/CCR7 enhances the proliferation, migration, and invasion of human bladder cancer t24 cells. PloS one 10: e0119506

Peled A, Abraham M, Avivi I, Rowe JM, Beider K, Wald H, Tiomkin L, Ribakovsky L, Riback Y, Ramati Y (2013) The highaffinity CXCR4 antagonist BKT140 is safe and induces a robust mobilization of human $CD34^+$ cells in patients with multiple myeloma. Clin Cancer Res 20:469–479

Peng C, Zhou K, An S, Yang J (2015) The effect of CCL19/CCR7 on the proliferation and migration of cell in prostate cancer. Tumor Biol 36:329–335

Phosrithong N, Ungwitayatorn J (2010) Molecular docking study on anticancer activity of plant-derived natural products. Med Chem Res 19:817–835

Porath D, Riegger C, Drewe J, Schwager J (2005) Epigallocatechin-3-gallate impairs chemokine production in human colon epithelial cell lines. J Pharmacol Exp Ther 315:1172–1180

Repasky MP, Shelley M, Friesner RA (2007) Flexible ligand docking with Glide. Curr Protoc Bioinformatics:8.12. 11-18.12. 36.

Roche DB, Buenavista MT, Tetchner SJ, McGuffin LJ (2011) The IntFOLD server: an integrated web resource for protein fold recognition, 3D model quality assessment, intrinsic disorder prediction, domain prediction and ligand binding site prediction. Nucleic Acids Res 39:W171–W177

Roell D, Baniahmad A (2011) The natural compounds atraric acid and N-butylbenzene-sulfonamide as antagonists of the human androgen receptor and inhibitors of prostate cancer cell growth. Mol Cell Endocrinol 332:1–8

Sanford DE, Belt BA, Panni RZ, Mayer A, Deshpande AD, Carpenter D, Mitchem JB, Plambeck-Suess SM, Worley LA, Goetz BD (2013) Inflammatory monocyte mobilization decreases patient survival in pancreatic cancer: a role for targeting the CCL2/CCR2 axis. Clin Cancer Res 19:3404–3415

Sarkar FH, Li Y (2006) Using chemopreventive agents to enhance the efficacy of cancer therapy. Cancer Res 66:3347–3350

Sawadogo WR, Boly R, Cerella C, Teiten MH, Dicato M, Diederich M (2015) A survey of marine natural compounds and their derivatives with anti-cancer activity reported in 2012. Molecules 20:7097–7142

Sawadogo WR, Schumacher M, Teiten M-H, Cerella C, Dicato M, Diederich M (2013) A survey of marine natural compounds and their derivatives with anti-cancer activity reported in 2011. Molecules 18:3641–3673

Schimanski CC, Bahre R, Gockel I, Junginger T, Simiantonaki N, Biesterfeld S, Moehler M (2006) Chemokine receptor CCR7 enhances intrahepatic and lymphatic dissemination of human hepatocellular cancer. Oncol Rep 16:109–113

Senthilkumar K, Manivasagan P, Venkatesan J, Kim SK (2013) Brown seaweed fucoidan: biological activity and apoptosis, growth signaling mechanism in cancer. Int J Bio Macromol 60:366–374

Shivakumar D, Williams J, Wu Y, Damm W, Shelley J, Sherman W (2010) Prediction of absolute solvation free energies using molecular dynamics free energy perturbation and the OPLS force field. J Chem Theory Comput 6:1509–1519

Singh P, Bast F (2014a) *In silico* molecular docking study of natural compounds on wild and mutated epidermal growth factor receptor. Med Chem Res 23:5074–5085

Singh P, Bast F (2014b) Multitargeted molecular docking study of plant-derived natural products on phosphoinositide-3 kinase pathway components. Med Chem Res 23:1690–1700

Singh P, Bast F (2015a) High-throughput virtual screening, identification and in vitro biological evaluation of novel inhibitors of signal transducer and activator of transcription 3. Med Chem Res 24:2694–2708

Singh P, Bast F (2015b) Screening and biological evaluation of myricetin as a multiple target inhibitor insulin, epidermal growth factor, and androgen receptor; *in silico* and *in vitro*. Invest New Drugs 33:575–593

Singh P, Bast F (2015c) Screening of multi-targeted natural compounds for receptor tyrosine kinases inhibitors and biological evaluation on cancer cell lines, *in silico* and *in vitro*. Med Oncol 32:1–18

Tabuchi M, Hayakawa S, Honda E, Ooshima K, Itoh T, Yoshida K, Park A-M, Higashino H, Isemura M, Munakata H (2013) Epigallocatechin-3-gallate suppresses transforming growth factor-beta signaling by interacting with the transforming growth factor-beta type II receptor. World 3:100–107

Takanami I (2003) Overexpression of CCR7 mRNA in nonsmall cell lung cancer: correlation with lymph node metastasis. Int J Cancer 105:186–189

Yuan Y (2014) Natural product chemokine receptor antagonists: what mother nature has offered us?. Curr Top Med Chem 14:1619–1634